DECAY OF PULSAR'S MAGNETIC FIELDS VIA NEUTRINO EMISSION PROCESSES

A THESIS SUBMITTED TO
THE SCHOOL OF GRADUATE STUDIES OF
ADDIS ABABA UNIVERSITY
IN PARTIAL FULFILLMENT OF THE
REQUIREMENTS FOR THE DEGREE OF
MASTER OF SCIENCE IN PHYSICS

BY
Tsegay Bezabh Buru

ADDIS ABABA UNIVERSITY
ADDIS ABABA, ETHIOPIA
OCTOBER, 2017

ADDIS ABABA UNIVERSITY
DEPARTMENT OF PHYSICS

The undersigned hereby certify that they have read and recommend to the Faculty of Science, School of Graduate Studies for acceptance a thesis entitled "**DECAY OF PULSAR'S MAGNETIC FIELDS VIA NEUTRINO EMISSION PROCESSES**" by **Tsegay Bezabh Buru** in partial fulfillment of the requirements for the degree of **Master of Science**.

Dated: October, 2017

Advisor: _____
Remudin Reshid(PhD)

Examiner: _____
Teshome Senbeta(PhD)

_____
Tilahun Tesfaye(PhD)

ADDIS ABABA UNIVERSITY

Date: **October, 2017**

Author: **Tsegay Bezabh Buru**

Title: **DECAY OF PULSAR'S MAGNETIC FIELDS VIA NEUTRINO EMISSION PROCESSES**

Department: **Physics**

Degree: **M.Sc.** Convocation: **October** Year: **2017**

Permission is herewith granted to Addis Ababa University to circulate and to have copied for non-commercial purposes, at its discretion, the above title upon the request of individuals or institutions.

Signature of Author

Dedication

This work is dedicated to my family

Table of Contents

List of Tables

List of Figures

Acknowledgements

First of all, thanks to God from the bottom of my heart who help me in any success in my life. God is with me every where. Next, I would like to express my heartfelt gratitude to my previous advisor Dr. Legesse Wotro Kebede and my current advisor Dr. Remudin Reshid for their unbounded assistance and encouragement, logical and technical guidance and enthusiastic approach. Their tireless follow up and their consistent support will be in my memory forever.

I am also indebted to Dr. Tadesse Desta, Tesfay Gidey, Tesfay Birhane and Ataklti Abrha for their invaluable assistance, comments and suggestions. Additional thanks go to my friends Ayalew, Alula, and Tesfay. Thank you for your valuable friendship, for meeting with me for lunches, dinners, movies, and for all the fun we had together. You are like my family and your special friendship and support had been crucial fuel for me to get through all the graduate years.

I thank the physics department of Addis Ababa University: Dr. Teshome, Dr. Ytagesu, Dr. Deribie, Dr. Belayneh, and Dr. Kenate. I would like to thank also the Ministry of Education.

Lastly, but not the least, I am very much grateful to my wife Nevayt Haftom and my daughter Emanda Tsegay for their valuable support and kind heartedly entertainment.

Tsegay Bezabh Buru
Addis Ababa, Ethiopia
October, 2017.

Abstract

Currently, there is no clear understanding of how pulsar magnetic fields decay. This is the motivation behind the development of this particular model for pulsar field dissipation. In this work we develop a theoretical model for surface magnetic fields of neutron stars (NSs) based on spinning separated charges that arise as a result of plasma diffusion processes inside NS matter [1]. As was described in this model, we have pointed out that such kinds of magnetic fields will be temperature dependent, and should decay primarily as a result of neutrino emissions. In this work we have formulated magnetic field decay law associated with neutrino emission process correspondingly the NSs cooling curve. Based on the above model, the magnetic field derived from this law is shown to be consistent with observations from typical young pulsars, like crab and vela young ones. We have also explored the possible implications of the results such as the observed variations and possible time evolution of pulsar braking indices are also discussed.

Chapter 1

Introduction

At present there is no, as such, a satisfactorily self-consistent theory for the origin of NS magnetic fields. The current understanding is that it can either be a fossil remnant (the standard picture) or it may be generated by surface thermal processes soon after the formation of the NS [2]. Models for field decay may follow either of these venues. Very recently, however, in another line of the theoretical research work separated charges have been suggested as likely sources for NS magnetic fields [1, 3]. According to [1], it has been shown that charge diffusion driven by the huge plasma density gradient, inherent to NS matter, results in separated charges large enough to generate surface magnetic fields which, very early in the life time of a typical NS, are at least 2 orders of magnitude stronger than those usually observed from young pulsars such as the Crab or Vela pulsar ($\sim 10^{12}$ G). Also, in the earlier work by the same author [3], it was demonstrated that the new model for NS surface of the star which give rise to dynamical properties of the magnetic moment that are not, in any form, predicted by the standard theory of pulsars. In this particular issue, the author was able to utilize these extra dynamical features to successfully address such points. These issues have been subjects of intense research for decades. For works performed

in this line see for example [4].

Investigations indicate that no significant magnetic decay occurs in a NS life time [5, 6]. This raises a serious question of how magnetic moments of so the called millisecond pulsars (MPs) and Low-Mass X-ray Binaries (LMXBs) decay from a typical value of $\sim 10^{30}$ G cm^3 down to 10^{25-26} G cm^3 in a time window of about 10^{7-8} yr [6, 7, 8, 9]. Obviously, Ohmic decay alone can not be responsible for the indicated magnetic moment. In fact, whether or not magnetic moments of pulsars undergo Ohmic decay is still an open question [10]. There are even those who hold that Ohmic decay is suppressed (by several orders of magnitude) due to space-time curvature effects, especially in older pulsars [11]. This problem has recently prompted a series of semi-empirical models for magnetic moment decay [12], including such approaches as the one involving mass-accretion induced decay scenarios [13]. However, NS magnetic fields decay as a result of neutrino and photon emissions lead to the cooling of NS in general. According to this model all form of radiations resulting in the spin down of the pulsar are also responsible for field dissipation [1].

Based on the new model for NS magnetic fields adopted in this work, a pair of decay laws for surface magnetic fields of young as well as old pulsars will be formulated. The two decay laws correspond respectively to the neutrino and photon emission branches of a typical NS cooling curve. However, the purpose of this paper is to point out that, the decay law due to neutrino emission a typical NS cooling curve lead to pulsar surface magnetic fields which is very much consistent with observations.

Finally, implications of the results to the time evolution of pulsar braking indices as well as their variations will be discussed.

Chapter 2

Pulsars and temperature dependence of their magnetic fields

2.1 Pulsars

According to their magnetic fields, NSs are classified into two, namely, pulsars and magnetars with typical polar surface magnetic fields of 10^{12-13} G and 10^{14-15} G, respectively [14]. Pulsars are rapidly rotating highly magnetized NSs that were first discovered in 1968 at radio wavelengths [15]. They emit periodic, non-thermal radiation by converting their rotational energy into dipole radiation. Pulsars are subdivided into Crab pulsar, Vela pulsar, etc. [14]. The Crab Nebula is a pulsar wind nebula system, and it is considered as the standard candle of gamma-ray astronomy due to its strong and steady emission. Pulsar wind nebula (PWN) are one type of supernova remnants (SNRs). These objects have a rapidly spinning NS, a pulsar, in their center and a nebula around it, which has strong non-thermal radio to gamma-ray emission. Magnetars are also subdivided into soft gamma repeaters (SGRs) and anomalous X-ray pulsars (AXPs) [16]. Magnetars are the most strongly-magnetized objects yet known in the universe. As already mentioned, the observationally inferred dipole magnetic fields of NSs, particularly magnetars (B $\sim 10^{14-15}$ G), are the

strongest known in the Universe, far exceeding any produced so far on Earth (up to 10^7 G produced in explosions, for very short times) or on other stars (up to 10^9 G on White dwarfs). An interesting comparison on magnetars is given on table (2.1) [16].

On the other hand, NSs share with White dwarfs and Upper main sequence stars the properties of being mostly or completely nonconvecting and having fields appearing to be constant over long time scales and thus likely "frozen in" rather than being rearranged and regenerated by a dynamo process. Table 2.1 shows that the widely different sizes and observed magnetic field strengths among these three types of stars largely compensate to give quite similar maximum magnetic fluxes $\Phi_{\max} \sim 10^{17.5-18}$ G km^2 in each type.

Table 2.1: Stars with long-lived magnetic fields.

Star type	Upper main sequence	White dwarf	NS
Radius [Km]	$10^{6.5}$	10^4	10^1
Max. magnetic field $B_{\max}$[G]	$10^{4.5}$	10^9	10^{15}
Max. magnetic flux $\Phi_{\max} \equiv \pi R^2 B_{\max}$[G Km^2]	10^{18}	$10^{17.5}$	$10^{17.5}$

The presence of strong magnetic fields in pulsars has been theoretically predicted and measurements of the polarization of the radio emission have provided the experimental evidence for it. Magnetic field strengths of the order of 10^{12} G can be derived from the observed in X-ray spectra of pulsars, e.g. [17]. These extremely strong magnetic fields originate in the collapse of the progenitor star. The strong magnetic fields $\sim 10^{12}$ G associated with pulsar are believed to have been arised as a result of the decrease in radius of the progenitor stars which, during the process of core collapse, shrink by a factor of $\sim 10^5$ [1].

From the observational evidence, which shows the evolution of NS magnetic field is the evolutionary connection between young and old NSs. Young NSs appear to have

strong magnetic fields $\sim 10^{11-15}$ G ("classical" pulsars, radio pulsars, "magnetars", X-ray pulsars). Older NSs are observed as recycled pulsars, such as MSPs and LMXBs. Their surface fields are weaker, $\leq 10^{10}$ G [1]. This weaker fields with older object suggests that the magnetic fields of NSs are subject to decay. Since the NSs found in MSPs and LMXBs have accreted substantial amounts of matter, but it is difficult to resolve whether the decay results from age or accretion [18]. Evidence favoring age comes from some statistical studies of ordinary, single, radio pulsars which conclude that the magnetic fields of these objects decay on time scales of order 10^7yr [5]. However, other studies reach the opposite conclusion [6]. The detection in $\gamma - ray$ burst spectra of what appear to be cyclotron lines formed in $(10^{12} - 10^{13})$ G fields [19] would provide evidence in favor of accretion, should the bursts emanate from old NSs [12].

If these two groups have an evolutionary connection, their dipole moment must decay [20]. The reduction in the magnetic dipole moment may be a direct or indirect consequence of the accretion process, or just an effect of age.

Studies of the pulsar distribution on the $\mathrm{P}-\dot{\mathrm{P}}$ diagram have lead to the claim that the magnetic torque decays on a time scale comparable to the life span of "classical" pulsars [21]. But was later put in doubt by other authors see e.g., [6], whose more careful analysis leads to opposite.

Our model for NS magnetic fields adapted in this work not only identifies the fields as being dipolar and successfully links the dynamical properties of the magnetic moment of the star to measured pulsar statistics, but it also indicates that these surface fields 'decay' through time as a result of a mechanism which is radically

different from that of Ohmic (spontaneous) decay commonly used to address situations involving the time evolution of pulsar fields. Even though, Ohmic decay is very slow and ineffective, more or less it could be counted as marginally responsible for field dissipation. Our model for NS magnetic fields adopted in this work is different, basically, because, unlike the fossil fields in the standard theory, the surface fields, in this case, are temperature dependent [see Eqn. (4.2.1)]. These fields are expected to 'decay' as a result of neutrino and photon emissions. However, since the cooling curves for typical NSs are known to have two different branches [22], related to the neutrino dominated and photon dominated cooling periods respectively.

The decay law predicted by the present theory will have two distinct segments, one corresponding to each branch. According to standard cooling calculations, the first branch of the cooling curve will cover the first $10^4 - 10^5$ yr. The first segment of the decay law corresponding to this branch can be shown to suggest a relatively slow decay rate. As a result, an initial surface magnetic field of, say, $\sim 10^{14}$ G will only fade away to $\sim 2 \times 10^{12}$ G in the first $\sim 10^4 - 10^5$ yr [22]. It is to be noted that active pulsars in the galaxy have surface magnetic fields in the range of $\sim (2 - 6) \times 10^{12}$ G. It is not our intention to study this issue here, but the second segment of the decay law, on the other hand, is expected to involve a much faster decay rate as compared to the first. This is due to the strong surface fields which naturally tend to enhance cooling by photons [22].

2.1.1 Pulsar's properties

Radio pulsars are regularly pulsating sources of radio waves, interpreted as magnetized, rotating NSs [23]. The present catalog of radio pulsars extends to more than 1400 objects, some of them are, Crab, PSR B1509-58, Vela, PSR B1706-44, PSR

B1951+32, Geminga, and PSR B1055-52, are list in Fig (2.1). Magnetic fields of radio pulsars, as measured by their periods, P and period derivatives, $\dot{P}$, fall into a broad range between $(10^8 - 10^{13})$ G [20, 24, 25]. According to their age t and their magnetic fields B, radio pulsars are also categorize in to two significantly different groups.

(i). young (t $\sim 10^{3-7}$ yr), relatively slow (P $\sim$ 16 ms to several seconds), and their magnetic fields of such pulsars that lie in the range $(10^{11} - 10^{13})$ G, strongly magnetized "classical" pulsars, and

(ii). old (t $\sim 10^{8-10}$ yr), fast (P $\sim$ 1.55ms to several ms), fields of recycled pulsars occupying the range $(10^8 - 10^{10})$ G, weakly magnetized "millisecond" pulsars.

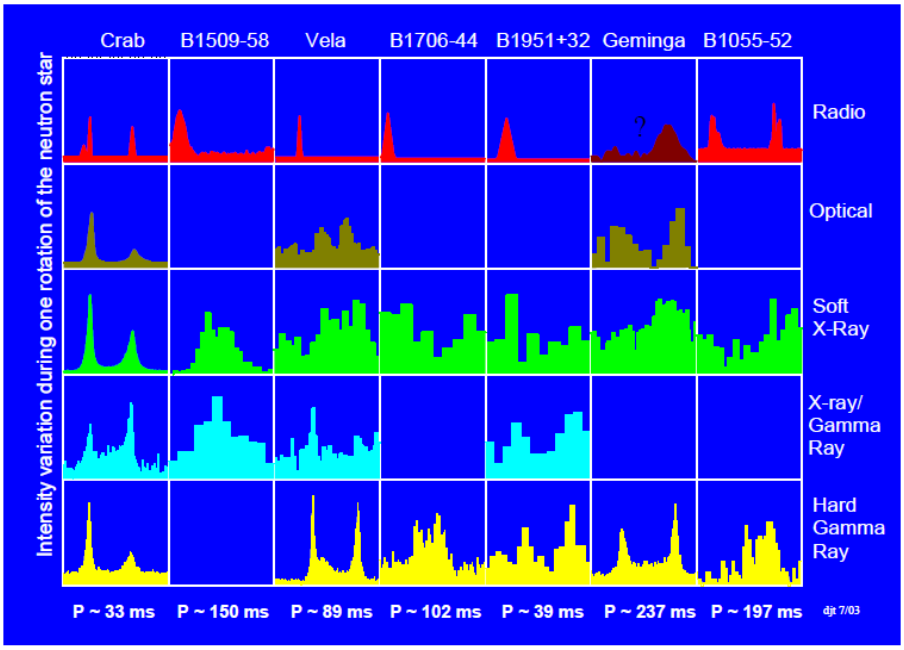

Figure 2.1: Light curves of seven gamma-ray pulsars in five energy bands, from left to right in order of characteristic age .

In Fig (2.1) we consider Light curves of seven gamma-ray pulsars in different

energy bands. These Gamma-ray Pulsars are Crab, PSR B1509-58, Vela, PSR B1706-44, PSR B1951+32, Geminga, and PSR B1055-52. Each pulsar shows one full rotation of the NS. [26]. These pulsar light curves (gamma-ray pulsars) are not the same at all wavelengths. Some combination of the geometry and the emission mechanism is energy dependent. In soft X-rays, for example, the emission in some cases appears to be thermal, probably from the surface of the neutron star; thermal emission is not the origin of radio or gamma radiation. The six pulsars seen by high-energy gamma rays all have a common feature they show a double peak in their light curves. Image credit: D. J., Thomson (NASA/GSFC) [26].

It is now generally accepted that pulsars are rapidly rotating NSs. In addition to being radio sources, pulsars radiate even more energy in the form of invisible "winds". The Crab Nebula is a supernova remnant that is lit up by the pulsar in its center, as best as one can tell [14]. The remnant of the Crab supernova, some nine hundred years after the explosion, is both accelerating and radiating in radio, optical, X-ray, and Gamma-ray bands powered by an energy input from the pulsar of $\sim 4\times10^{31}$J s^{-1}. By equating the input in the nebula to the power loss of the magnetic dipole radiation Eqn. (2.1.6), one can derive the magnetic field. Consider the fastest rotating pulsar with a period $\sim$ 33 ms, PSR 1937+21 [27]. Now we can find the magnetic field

$$\frac{B_p^2 R^6 \Omega^4 \sin^2\alpha}{6c^3} = 4\times10^{31}\frac{J}{s}, \tag{2.1.1}$$

where B_p is the dipolar magnetic field at the stellar pole, R is a canonical NS radius ($\sim$ 10 km), Ω is the angular velocity, c is the speed of light and α is the angle of inclination of the magnetic axis to the rotational axis.

From the above relationship we can compute an expression for magnetic field,

$$B_p = \sqrt{\frac{4\times6\times10^{31}c^3}{R^6\Omega^4\sin^2\alpha}}\ \text{J s}^{-1}, \tag{2.1.2}$$

where P $\sim$ 33 ms is the observed period, c $= 3 \times 10^8$ m s^{-1}, assuming $\alpha = 90^o$, and replacing Ω by $\frac{2\pi}{P}$, we can obtain

$$B_p \approx 4 \times 10^{12} \text{ G}. \tag{2.1.3}$$

According to the proponents of this model Gold [23], suggested that the radio signals from a NSs are caused by the magnetic fields around the star. When a NS is rotating, carrying a strong dipolar magnetic field with it, it acts as a very energetic electric generator, and provides a source of energy for radiation.

Classical electrodynamics predicts that a time varying magnetic dipole moment $\vec{m}$ results in a loss of energy described by the Larmor formula [28].

$$P = \dot{E} = \frac{2}{3c^3} \mid \ddot{\vec{m}} \mid^2, \tag{2.1.4}$$

here dots indicate that time derivative.

A magnetic dipole moment, forming an angle α with the rotation axis, is written as

$$\vec{m} = \frac{B_p R^3}{2} \sin\alpha \; e^{(i\Omega t)} \hat{z}, \tag{2.1.5}$$

where $\hat{z}$ is the unit vector aligned to the spin vector and $\mid \vec{m} \mid = \frac{1}{2} B_p R^3$. Then ,for a rotating dipolar field, the radiation using the Larmor formula is

$$P = \dot{E} = \frac{B_p^2 R^6}{6c^3} \Omega^4 \sin^2\alpha, \tag{2.1.6}$$

where $\vec{\Omega}$ is the angular velocity, α the angle between $\vec{m}$ and $\vec{\Omega}$. Since the energy is being lost, Gold [23] predicted that the rotation period of the NS will increase and the rate of increase would be

$$\frac{d}{dt}\left(\frac{1}{2} I \Omega^2\right) = -\dot{E}, \tag{2.1.7}$$

where I represent the moment of inertia of NS. Assuming the moment of inertia I is independent of time , so that

$$I\Omega\dot{\Omega} = -\dot{E}, \tag{2.1.8}$$

$$\dot{\Omega} = \frac{\dot{E}}{I\Omega} = \frac{B_p^2 R^6}{6c^3 I}\Omega^3 \sin^2\alpha. \tag{2.1.9}$$

In 1975, when the Crab Pulsar was discovered, a slow increase of the period was detected. At that time, the period of the Crab Pulsar was 33 ms, for atypical moment of inertia I $\sim 10^{45}$ g cm^2 and the rate of increase of the period was $\dot{P} = 1.2589 \times 10^{-15}$. If we assume this increase of the period is due to the radiation of the magnetic dipole, then B_p should be about 5×10^{12} G. Thus, the increase of the period of the Crab pulsar suggests the presence of strong magnetic fields associated with NSs. Thus, it is in a good agrement what we have been shown in Eqn. (2.1.3)

2.1.2 Braking index of pulsars

In the previous section it was already pointed out that the rotation angular frequency (Ω) of the pulsar changes with time. Just like in the case of the magnetic field, the fast rotation originates in the collapse of the progenitor star. Angular momentum is conserved. Since the discovery of the first pulsar in 1968, the experimental techniques have improved significantly and have allowed for precise measurements of the pulsar period for many pulsars. For most of the pulsars, it is also possible to measure the time derivative of the pulsar angular frequency ($\dot{\Omega}$), and for some of the pulsars, the second and third derivative of the angular frequency, is also measurable. The change in the rotation angular frequency is related to the braking index n, which is defined as

$$\dot{\Omega} = -K\Omega^n, \tag{2.1.10}$$

assuming K is constant. The braking index of a pulsar can directly be calculated if the second derivative of the angular frequency ($\ddot{\Omega}$), can be measured. The braking index is then equal to

$$\mathrm{n} = \frac{\ddot{\Omega}\Omega}{\dot{\Omega}^2} = 2 - \frac{\ddot{\mathrm{P}}\mathrm{P}}{\dot{\mathrm{P}}^2}. \tag{2.1.11}$$

If one assumes that the loss of rotational energy is entirely converted into magnetic dipole radiation, then it follows from Eqn. (2.1.9) that

$$\dot{\Omega} \propto \Omega^3, \tag{2.1.12}$$

where in this case n = 3. We get an estimate of the pulsar age as

$$\tau_\mathrm{c} = -\frac{\Omega}{2\dot{\Omega}}. \tag{2.1.13}$$

Similarly

$$\tau_\mathrm{c} = \frac{\mathrm{P}}{2\dot{\mathrm{P}}}, \tag{2.1.14}$$

which is called the characteristic age (or spin down age) of the pulsar. In most cases, the characteristic age is stated under the implicit assumption of magnetic dipole radiation (n = 3). The characteristic age provides a good estimate for many pulsars, but there are also significant deviations found for pulsars, for which the true age is known from an association with a historical supernova. This may be due to a braking index $\mathrm{n} \neq 3$.

In Section (2.1.1) we have discussed the theoretical description of pulsar and spin-down energy radiation from a rotating dipole. Thus, using Eqns. (2.1.6) and (2.1.8), we have

$$\mathrm{P}\dot{\mathrm{P}} = \mathrm{K}\mathrm{B}_\mathrm{p}^2, \tag{2.1.15}$$

where $K = \frac{R^6(2\pi)^2 \sin^2\alpha}{6c^3 I}$. By substituting Eqn. (2.1.15) in to Eqn. (2.1.11), we get

$$n = 3 - \frac{P}{\dot{P}} \left(\frac{1}{KB_p^2} \right) \frac{d}{dt}(KB_p^2), \tag{2.1.16}$$

where the proportionality constant K in the Eqns. (2.1.15) and (2.1.16) includes different dependencies on the star radius, moment of inertia, magnetic field strength, and angle between rotation and magnetic axis. If all these quantities are constant in time, the magneto-dipole spin-down mechanism predicts a braking index n = 3 (see Eqn. (2.1.10) and (2.1.16)) but variations in time of any of these quantities may cause departures from this canonical value.

If KB_p^2 is constant in time, the braking index is n = 3. Most pulsars show strong deviations from n = 3, implying a time variation of KB_p^2 lead to different braking index. If the braking is due to a relativistic stellar wind, the braking index n = 1 [14]. The observed braking index n, which has been determined for several young radio pulsars, are all less than 3. For example, the braking index of the Crab pulsar PSR 0531+21 is 2.509 ± 0.001 [29], $n = 1.4 \pm 0.2$ for the Vela pulsar PSR 0833-45 [30]. For PSR B1509-58, $n = 2.837 \pm 0.001$ [31]. Clearly, the braking index deviates from what would be the expectation for pure magnetic dipole radiation. One explanation for this is, that the energy flow from the pulsar is not only by electromagnetic radiation, but does also have a contribution from the particle outflow. Since the magnetic field dominates the physics of the outer magnetosphere, Eqn. (2.1.6) will still give a good approximation of the total energy flow.

In previous works, many authors proposed various models to explain the discrepancy between observed and theoretical predicted value of n suggested that neutrino and photon radiation coming from superfluid neutrons may brake the pulsars. [32] proposed that $n < 3$ due to a multipole field and field evolution. The braking index

can be directly inferred from the measurement of the star frequency and its derivatives. It differ from one pulsar to another (see references in Kaspi) [33].

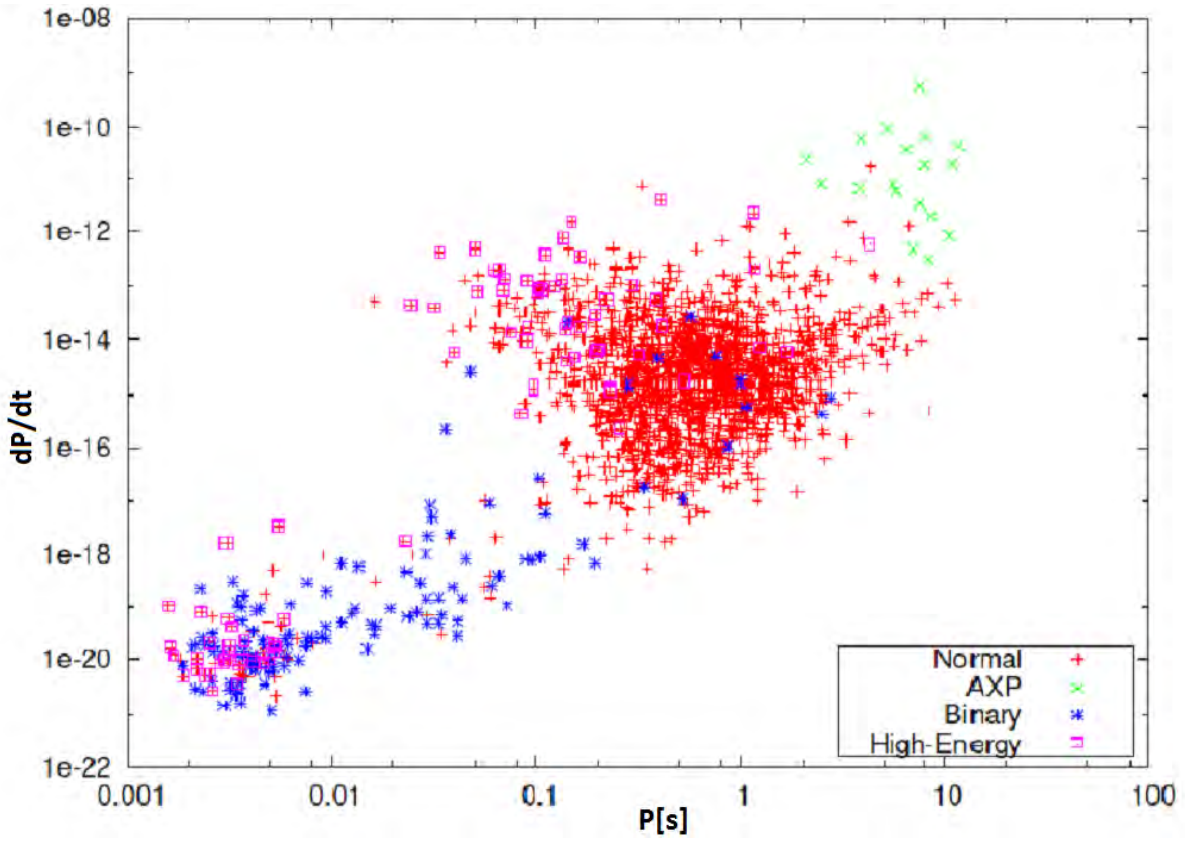

Figure 2.2: The P − Ṗ diagram shows the nature and evolution of detected pulsars.
.

Fig. (2.2) is a plot of the absolute value of the time derivative of pulse period (Ṗ), versus pulse period (P). It is useful for following the pulsar lives. It also encodes a great amount of information about the pulsar population and its properties, as determined and estimated from these two quantities. Special classes of pulsars are shown separately such as, Normal pulsars, Anomalous X-ray pulsars (AXP) or Soft Gamma-ray Repeaters with pulsations, high-energy pulsars with emitted frequencies between radio and infrared or higher, and binary pulsars. The diagram clearly shows

the distinction between "normal" pulsars and millisecond pulsars. The differences are due to the different ages and magnetic field strengths of these two populations. The plot shows that "normal" pulsars reside at the top right of the plot. These are young with strong magnetic fields (B $\sim 10^{12}$ G), large pulse period (P), and large period derivative ($\dot{\mathrm{P}}$) . Whereas, located at the bottom left are millisecond pulsars. These are much older with weaker magnetic fields (B $\sim 10^{8}$ G), smaller pulse period (P) and period derivative ($\dot{\mathrm{P}}$). At birth pulsars appear in the upper left corner of the diagram; if the magnetic field B is conserved, they gradually move to the right and down, along lines of constant B. The pulsars occupy the largest region of the diagram with their population extending from the very short period, low $\dot{\mathrm{P}}$ millisecond pulsars up to high $\dot{\mathrm{P}}$, high magnetic field pulsars that border the magnetar range. The magnetars have the highest $\dot{\mathrm{P}}$. Figure generated using data available from [34].

2.2 Temperature dependence of pulsar's magnetic fields

Just recently it has been indicated that plasma density gradients inherent to NS matter could lead to large scale plasma diffusion and subsequent charge separation with excess negative charge accumulating in the crust while at the same time, almost the same amount of excess positive charge is left behind at the solid core. Surface magnetic fields are then expected from the spinning of these separated charges. Below is given a formal discussion on the processes of plasma diffusion in a two-component degenerate, dense Fermi system representative of the NS matter we are considering. This is variant to the elementary approach we used in the original paper [1]. Ignoring the temperature gradient driving force for reason of high conductivity of the NS

matter, in this case currents of the charge carriers can be modeled as [1].

$$\mathrm{n}_i = -\mathrm{D}^0(\partial_{\mathrm{i}}\mathrm{n}_0 - \Gamma^0_{0\mathrm{i}}\mathrm{n}_0) + \mu\mathrm{n}_0\mathrm{g}_{\beta\mathrm{i}}\mathrm{F}^{0\beta}, \tag{2.2.1}$$

where $\mathrm{n}_\alpha \equiv (\mathrm{n}_0, \mathrm{n}_{\mathrm{i}})$ is the four-particle current, n_0 is the local current density, $\mathrm{g}_{\beta\mathrm{i}}$ is the metric tensor, $\mathrm{F}^{\alpha\beta}$ is electromagnetic field tensor and D^0 is the diffusion coefficient which we take as scalar.

The four-vector diffusion coefficient D^α defined by

$$\mathrm{D}^\alpha = \mathcal{H}(\mathrm{p}^\alpha - \mathrm{m}_{\mathrm{o}}), \tag{2.2.2}$$

where p^α is the four-vector momentum, $\mathcal{H}$ is the total hamiltonian of the particle and m_{o} is the rest mass of the particle. The factor $(\mathrm{p}^0 - \mathrm{m}_{\mathrm{o}}) \propto \mathrm{K_B T}$ (by equipartition principle) is expected to be the energy corresponding to the particle's random motion responsible for the various scattering that determine the different transport coefficient of the system including the diffusion coefficient and the mobility of the individual species making up the plasma. $\mathrm{K_B}$ is the Boltz-mann constant and T is the internal temperature of the NS.

Normally the electrons, due to their small masses, are much more responsive and quick as compared to the protons and therefore dominate the diffusion process. The electron-proton interaction can be considered as the long-range Coulombic interaction. Standard calculation for dense Fermi system show that [35, 36]

$$\mathcal{H} \sim \frac{\pi^2\hbar^6}{\mathrm{m}^{*4}_{\mathrm{e}}\mathrm{K}^2_{\mathrm{B}}\mathrm{T}^2}, \tag{2.2.3}$$

and

$$\mu_{\mathrm{e}} \sim \frac{\mid \mathrm{e} \mid \pi^2\hbar^6}{\mathrm{m}^{*2}_{\mathrm{e}}\mathrm{m}^{*2}_{\mathrm{p}}\mathrm{K}^2_{\mathrm{B}}\mathrm{T}^2}, \tag{2.2.4}$$

where m_e^* and m_p^* are effective electron and proton masses, respectively and $\mid e \mid$ is the absolute magnitude of the electron charge.

By considering the dipolar component, we will derive the electric field due to the space charge created as a result of the diffusion process by assuming model Eqn (2.2.1) taken at equilibrium and in the absence of gravity. Thus, Eqn. (2.2.1) will reduce to

$$0 = -D^0(\partial_i n_0) + \mu n_0 g_{\beta i} F^{0\beta}. \tag{2.2.5}$$

The electro magnetic field tensor is defined as [37]

$$F^{\alpha\beta} = \begin{pmatrix} 0 & \frac{E_x}{c} & \frac{E_y}{c} & \frac{E_z}{c} \\ -\frac{E_x}{c} & 0 & B_z & -B_y \\ -\frac{E_y}{c} & -B_z & 0 & B_x \\ -\frac{E_z}{c} & B_y & -B_x & 0 \end{pmatrix} \tag{2.2.6}$$

Under Post-Newtonian approximation the metric tensors can be expanded as [37]

$$g_{00} = -1 + \overset{2}{g}_{00} + \overset{4}{g}_{00} + ...$$

$$g_{ij} = \delta_{ij} + \overset{2}{g}_{ij} + \overset{4}{g}_{ij} + ...$$

and

$$g_{i0} = \overset{3}{g}_{i0} + \overset{5}{g}_{i0} + ... \tag{2.2.7}$$

By using Eqns. (2.2.5) - (2.2.7), it is clear to write

$$D^0(\partial_i n_0) = \mu n_0(\delta_{ki} + \overset{2}{g}_{ki} + ...)F^{0k}. \tag{2.2.8}$$

If we approximate the metric tensors to their first term we will get the following

$$D^0(\partial_i n_0) = \mu n_0(\delta_{ki} F^{0k}), \tag{2.2.9}$$

here if k = i, then $\delta_{ki} = 1$, having this Eqn. (2.2.9) will become

$$D^0(\partial_i n_0) = \mu n_0 F^{0i}, \tag{2.2.10}$$

here the field tensor F^{0i} is obtained from Eqn. (2.2.6)

$$F^{0i} = \frac{E(r)}{c} = \frac{E_x}{c} + \frac{E_y}{c} + \frac{E_z}{c}, \tag{2.2.11}$$

where, $F^{01} = \frac{E_x}{c}$, $F^{02} = \frac{E_y}{c}$ and $F^{03} = \frac{E_z}{c}$, here, c is unity. By substituting Eqn. (2.2.11) in to Eqn. (2.2.10) will provide the electric field due to the space charge created as a result of the diffusion process as

$$E(r) \simeq \frac{D_e^0}{\mu_e}\left(\frac{1}{n_0}\frac{\partial n_0}{\partial r}\right). \tag{2.2.12}$$

Normally gravitational fields are so weak as compared to electro static driving forces, by factor of $\sim 10^{-11}$, that is why different authors ignore this field in their discussions about NSs. Thus, in calculating the magnitude of the separated charges and the resulting dipole fields, Kebede, [1] ignored gravity. In the absence of gravity we expect to have dipolar surface fields for NSs as shown in Fig. (2.3).

The charged particles will move along the $\vec{B}$ field lines. There are two kinds of $\vec{B}$ field lines, one is open and the other is closed, as shown in Fig. (2.3). The field lines 1, 2, 3 and 1', 2', 3' are closed field lines and the filed lines O and O' are open. When the particles are moving along the closed field lines, they will eventually come back to the stellar surface. When the particles are moving along the open field lines, they will form beamed winds.

Until recent years, it was believed that, the NS magnetic field is mainly dipolar and different authors discuss about pulsars based on this kind of field. However, there will introduce small non-dipolar components to the pulsar surface magnetic

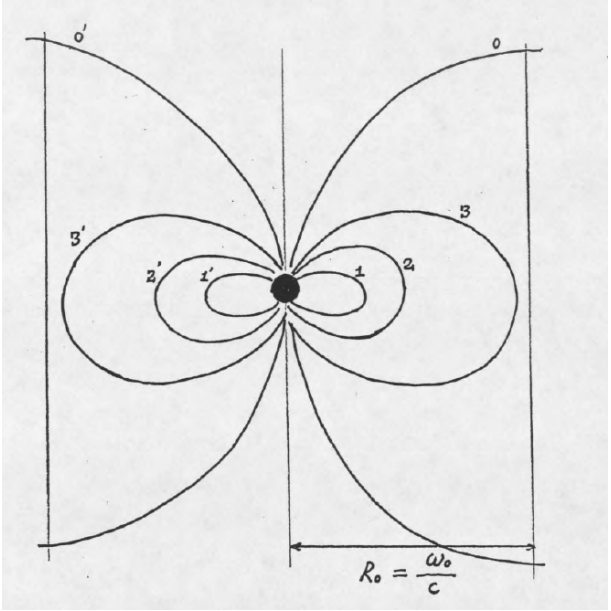

Figure 2.3: Illustration of dipolar magnetic field

field which otherwise is mainly dipolar as predicted by our model [1]. It is very well known that the magnetic dipole model accounts for many of the observed properties of pulsars [38]. The magnetic field of NSs are both dipolar and small non-dipolar components as [39]. Moreover, there are also suggestions by several authors [4, 40] that, in general, small non-dipolar components of pulsar fields could be responsible for the commonly observed braking index variations.

From Eqns. (2.2.2) - (2.2.4) follows the ratio of the diffusion coefficient to the mobility as

$$\frac{\mathrm{D_e^0}}{\mu_\mathrm{e}} \sim \left(\frac{\mathrm{m_p^*}}{\mathrm{m_e^*}}\right)^2 \frac{(\mathrm{P_e^0} - \mathrm{m_o^e})}{\mid \mathrm{e} \mid} \equiv \left[\left(\frac{\mathrm{m_p^*}}{\mathrm{m_e^*}}\right)^2 \frac{\mathrm{K_B T}}{\mid \mathrm{e} \mid}\right]. \tag{2.2.13}$$

This is the famous Einsteins relation corrected for e-e and p-e scattering. In the region of interest, the neutrons are in a superfluid state providing practically zero

scattering cross-section. We now remodel the plasma density gradient as [1]

$$\frac{\partial n_0}{\partial r} \sim \frac{1}{m_n}\frac{\partial}{\partial r}\left(\rho(r)\frac{n_p}{n_n}\right), \tag{2.2.14}$$

where m_n is the neutron rest mass, ρ(r) is the rest-mass density of the NS matter, $n_p(\sim n_0)$ and n_n are the proton and neutron number densities, respectively. Using Eqn. (2.2.14) and the appropriate proton to neutron density ratio for NS matter [37] we find, under an approximation of very high central density ($\rho_c > 10^{15}$ gm cm^{-3}), i.e.,

$$\frac{1}{n_0}\frac{\partial n_0}{\partial r} \sim \frac{1}{\rho_c}\frac{\partial \rho(r)}{\partial r}. \tag{2.2.15}$$

By substituting Eqns. (2.2.13) and (2.2.15) in to Eqn. (2.2.12) we provide the electric field due to the space charge in this case

$$E(r) \sim \frac{1}{\rho_c}\left(\frac{m_p^*}{m_e^*}\right)^2 \frac{K_B T}{|\,e\,|}\frac{\partial \rho(r)}{\partial r}. \tag{2.2.16}$$

From Eqn. (2.2.16), it is very important to point out that, E(r) is temperature dependent T.

Calculation of the separated (-/+) charges can now be made from application of Gauss' law to Eqn. (2.2.16) [1]. What is very important to notice in this case is the fact that the magnitude of the separated charges Q will be linearly dependent on the internal temperature T, i.e., Q $\propto$ T. The probability of getting an element of separated charge dq, produced by the diffusion process (naturally involves random scattering) in a given element of volume dV and in a time window of, say, equal to the average relaxation time of the electrons (τ), will diminish with the cooling of the NS due to adverse effects of mainly increasing viscosity $\eta(\eta \sim \frac{1}{\tau^2})$ [35, 41]. Most of the separated negative charge will naturally install itself very close to the NS surface and eventually spin along with the star. It is then a simple exercise Jackson (1975),

(Chap. 5, Prob. 7) [42], to evaluate the vector potential A_ϕ generated by the spinning negative charge and the related surface magnetic induction vector B. The latter is shown in the original paper to be dipolar and linearly dependent on the charge Q. This means that, just like the separated charge, the surface magnetic field will also be temperature dependent. It is important to note that the contribution of the inner dipole to the surface magnetic field of the NS is very small, smaller by a factor of $(r_o/R)^2$ than that from the outer dipole, where ($r_o \ll R$) is the radius of the inner solid core.

2.3 Summery

Eqn. (2.1.16) shows that any variation of B_p results in a deviation from the canonical value n = 3, standard value. For an increasing B_p we will always obtain $n < 3$, while $n > 3$ is the signature of a decreasing B_p. Different processes lead to different braking indices: a quadrupolar braking field (gravitational or magnetic) implies n = 5, while the ejection of an unmagnetized particle wind would result in n = 1. The braking index can be directly inferred from the measurement of the star frequency and its derivatives.

For the relativistic NS matter that we have assumed, there could be depending on the internal temperature of the star, enough separated charges that would, initially, give rise to dipolar surface magnetic fields. These fields are linearly dependent on the magnitude of the separated charges. The magnitude of the separated charges Q also linearly dependent on the internal temperature T, i.e., $Q \propto T$. This means that, just like the separated charge, the surface magnetic field will also be linearly dependent on the internal temperature, i.e., $B \propto T$. These fields are expected to 'decay' as a result

of neutrino and photon emissions. According to standard cooling calculations, the neutrino emission of the cooling curve will cover the first $10^4 - 10^5$ yr. In this situation the decay law corresponding to this branch can be shown to suggest a relatively slow decay rate. As a result, an initial surface magnetic field of, say, $\sim 10^{14}$ G will only fade away to $\sim 2 \times 10^{12}$ G in the first $\sim 10^4 - 10^5$ yr.

When a NS is rotating, carrying a strong dipolar magnetic field with it, it acts as a very energetic electric generator, and provides a source of energy for radiation. We are considering the dipolar component of NS magnetic field resulting from the rotation of the NS, by using Eqn. (2.2.1) and applying Post-Newtonian approximation.

In the next sections we will have discuss in details about the cooling theory and neutrino emission processes.

Chapter 3

Cooling theory and neutrino emission processes

3.1 Cooling theory

A NS is a product of supernova explosion. It is generally believed that NSs are formed at very high interior temperatures ($T \gtrsim 10^{11}$ K) in the core of a supernova explosion [43]. The predominant cooling mechanism immediately after formation is via neutrino emission from the entire stellar body, with an initial cooling timescale of seconds. After about a day, the internal temperature drops to $10^9 - 10^{10}$ K [22]. Also photon emission occurs at the stars surface. Photon emission overtakes neutrinos only when the internal temperature falls to $\sim 10^8$ K, with a corresponding surface temperature roughly two orders of magnitude smaller. Neutrino cooling dominates for at least the first 10^5 yr, and typically for much longer, in all standard cooling calculations performed recently. These theoretical calculations which provide curves of the neutron surface temperature as a function of time, which in principle are subject to observational verification [22].

In Fig. (3.1), we show the effects of magnetic field and temperature on NS core. The dot-dashed horizontal lines show the initial temperature (just after core collapse),

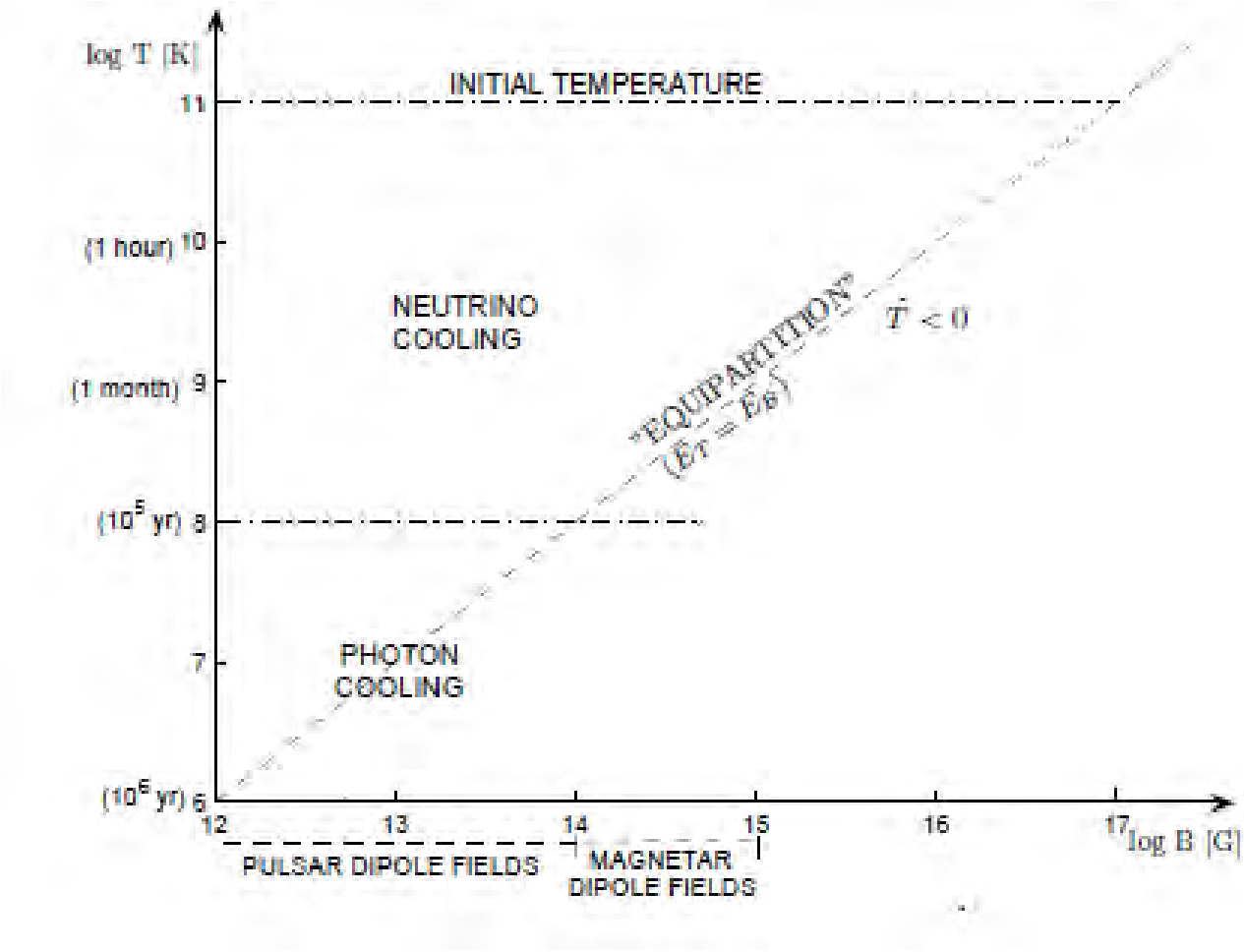

Figure 3.1: Magnetic field-temperature plane for NS core.

and the transition from neutrino-dominated (modified Urca) to photon-dominated cooling. The dashed diagonal line corresponds to the equality of magnetic and thermal energy. The star cools passively, on the time scales indicated in parenthesis along the vertical axis, without substantial magnetic field decay, so the evolution of the star is essentially a downward vertical line. (Figure prepared by C. Petrovich and first published in Ressenger) [44].

Qualitatively, one can distinguish three cooling stage. At the first ('non-isothermal')

stage ($t \lesssim 10^2$ yr) the main cooling mechanism is neutrino emission but the stellar interior stays highly non-isothermal. At the second ('neutrino') stage ($10^2 \lesssim t \lesssim 10^5$ yr) the cooling goes mainly via neutrino emission from isothermal interiors. At the third ('photon') stage ($t \gtrsim 10^5$ yr) a star cools predominantly through the surface photon emission.

The effects of strong magnetic fields on NS cooling have also been considered by a number of authors [22, 43, 45]. In the very early days, soon after the discovery of pulsars, the effects of magnetic fields on NS cooling were considered to be very important, in the sense that the presence of strong magnetic fields will keep the star hotter (at a given age), at least during the neutrino cooling era, see e.g., [46].

When the NS cooling problem was first calculated, the isothermal method was used [43]. The core temperature is determined by energy balance equation, during the neutrino cooling era.

$$C_\nu \frac{dT_c}{dt} = \varepsilon_\nu, \tag{3.1.1}$$

here T_c is the core temperature, C_ν is the specific heat, and ε_ν is the neutrino emissivity (= rate of energy loss by all neutrinos processes per unit mass). According to Tsuruta's docterial thesis [43] is a cooling profile of NS obtained with the isothermal method, we see that after the age of $t \sim 10^5$ yr, the surface temperature takes sudden drops. During the neutrino cooling era, i.e. before $t \sim 10^5$ yr, the stellar cooling rate is determined by the energy loss due to neutrino emission, while during the photon cooling era, i.e. after $t \sim 10^5$ yr, the stellar cooling rate is determined by the energy loss via photon emission.

The energy loss rate due to the neutrino emissions during modified URCA (MURCA)

reaction can be written approximately as [47]

$$L_\nu{}^{(\mathrm{MURCA})} \equiv 5.3 \times 10^{39}\ \mathrm{erg\ s^{-1}} \left(\frac{M}{M_\odot}\right) \left(\frac{\rho_{\mathrm{nuc}}}{\rho}\right)^{1/3} T_9^8, \tag{3.1.2}$$

here $T_9 = T/10^9$, M is neutron star mass, $M_\odot$ is solar mass, ρ is average density and ρ_{nuc} is the nuclear density ($\rho_{\mathrm{nuc}} = 2.8 \times 10^{14}\ \mathrm{gm/cm^3}$).

The total stellar energy content as [47]

$$E \equiv 6 \times 10^{47}\mathrm{erg} \left(\frac{M}{M_\odot}\right) \left(\frac{\rho}{\rho_{nuc}}\right)^{-2/3} T_9^2. \tag{3.1.3}$$

Using Eqns. (3.1.2) and (3.1.3) the energy balance requires that,

$$\frac{dE}{dt} = -L_\nu{}^{(\mathrm{MURCA})}. \tag{3.1.4}$$

Substituting Eqns. (3.1.2) and (3.1.3) into Eqn. (3.1.4), we obtain

$$T_9^{-7} \left(\frac{dT_9}{dt}\right) = -4.4 \times 10^{-9}\ \mathrm{s^{-1}} \left(\frac{\rho_{\mathrm{nuc}}}{\rho}\right)^{-1/3}. \tag{3.1.5}$$

Integrating the differential Eqn. (3.1.5) in order to relate temperature and time, we get:

$$T_9^{-6} = 2.64 \times 10^{-9}\ \mathrm{s^{-1}} \left(\frac{\rho_{\mathrm{nuc}}}{\rho}\right)^{-1/3} t + C, \tag{3.1.6}$$

here t is the age of the NS, C is an integration constant.

On the other hand, the energy loss rate due to the surface photon emission L_γ (photon luminosity = energy transport by photons per unit time) as [22, 46],

$$L_\gamma = 4\pi R^2 \sigma T_7^4 g_{00}^{-1}, \tag{3.1.7}$$

where g_{00} is the metric tensor as we have discussed in the previous section (§2.2), σ is the Stefan-Boltzmann constant and T_7 is the observable overall effective surface temperature related to the internal temperature T approximately by [45, 46].

$$T_7 = 4.648 \times T^{2/3} = (10\ T)^{2/3}. \tag{3.1.8}$$

After some calculations, we obtain the cooling rate due to the photon emission as:

$$\mathrm{T}^{-2/3} = 4.648 \times 10^{-4} \left(\frac{\mathrm{M}}{\mathrm{M}_{\odot}} \right)^{-1/3} \mathrm{t} + \mathrm{C}. \tag{3.1.9}$$

Before the age $\mathrm{t} \sim 10^5$ yr, the MURCA process dominates the photon emission, while after $\mathrm{t} \sim 10^5$ yr, the photon cooling takes over. Thus, at higher temperatures, the MURCA process is more important than the photon cooling [45].

3.2 Neutrino emission processes

Neutrino is an elementary particle with no (or very little) mass and no electric charge that travels at the speed of light and carries energy away during certain types of nuclear reactions [47]. The most powerful neutrino emission is produced in the stellar core, in which the typical neutrino energies in nonsuperfluid stars are $\sim \mathrm{k_B T}$ [48].

Neutrino emission is generated in numerous reactions in the interiors of NSs. When the neutrinos pass through a NS, there, are two kinds of reactions between the neutrinos and the NS matter: charged current interactions and neutral current interactions as reviewed for instance by [48].

(i). The charged current interactions are the following three reactions

$$\nu_{\mathrm{e}} + \mathrm{n} \rightarrow \mathrm{p} + \mathrm{e}^{-}, \tag{3.2.1}$$

$$\bar{\nu_{\mathrm{e}}} + \mathrm{p} \rightarrow \mathrm{n} + \mathrm{e}^{+}, \tag{3.2.2}$$

and

$$\bar{\nu_{\mathrm{e}}} + \mathrm{p} + \mathrm{n} \rightarrow \mathrm{n} + \mathrm{n} + \mathrm{e}^{+}, \tag{3.2.3}$$

where ν_{e} and $\bar{\nu_{\mathrm{e}}}$ stand for electron neutrino and antineutrino, respectively.

(ii). The neutral current interactions are

$$\mathrm{n} + \nu_{\mathrm{e}} \rightarrow \mathrm{n} + \nu_{\mathrm{e}}, \tag{3.2.4}$$

and

$$\mathrm{n} + \nu_{\mu} \rightarrow \mathrm{n} + \nu_{\mu}. \tag{3.2.5}$$

The electric neutrality requires the electron and proton number densities be equal, i.e., $(\mathrm{n_p} = \mathrm{n_e})$.

Furthermore, there are also another neutrino emission processes inside NSs, the neutrinos are produced both inside the core and in the crustal region. Inside the core, the basic processes are the MURCA process, and neutron-neutron and neutron-proton bremsstrahlung processes. Inside the crust, the major processes are the direct coupled electron-neutrino processes, plasmon-neutrino, photon-neutrino and electron-positron pair neutrino processes [49].

(i). The MURCA process proceeds as follows

$$\mathrm{n} + \mathrm{n} \rightarrow \mathrm{n} + \mathrm{p} + \mathrm{e}^{-} + \bar{\nu_{\mathrm{e}}}, \tag{3.2.6}$$

and

$$\mathrm{n} + \mathrm{p} + \mathrm{e}^{-} \rightarrow \mathrm{n} + \mathrm{n} + \nu_{\mathrm{e}}. \tag{3.2.7}$$

It is similar to the direct URCA, but involves an additional nucleon spectator. The additional nucleon is required to conserve momentum of the reacting particles; it will do the job even if the direct URCA is forbidden. The extra particle relaxes the momentum conservation condition but slows the reaction rate.

The direct URCA process, $\mathrm{n} \rightarrow \mathrm{p} + \mathrm{e}^{-} + \bar{\nu_{\mathrm{e}}}$, is usually considered as highly impossible inside the core of NSs, because of the energy restriction. But if there is a

bystander particle present to absorb the momentum of neutrons, a MURCA process is possible, as shown in Eqn. (3.2.6).

(ii). The nn and np bremsstrahlung processes are

$$\mathrm{n} + \mathrm{n} \rightarrow \mathrm{n} + \mathrm{n} + \nu_{\mathrm{e}} + \bar{\nu_{\mathrm{e}}}, \tag{3.2.8}$$

and

$$\mathrm{n} + \mathrm{p} \rightarrow \mathrm{n} + \mathrm{n} + \nu_{\mathrm{e}} + \bar{\nu_{\mathrm{e}}}. \tag{3.2.9}$$

In the absence of the direct URCA process, the standard neutrino luminosity is determined not only by the MURCA processes but also by the processes of neutrino bremsstrahlung radiation in nucleon-nucleon collisions. These reactions go via weak neutral currents and produce neutrinos of any favor; neutrino pairs are emitted in strong nucleon-nucleon collisions. In analogy with the MURCA process, the emissivities depend on the employed model of nucleon-nucleon interaction. Contrary to the MURCA, an elementary act of the nucleon-nucleon bremsstrahlung does not change the composition of matter.

The direct coupled electron-neutrino processes are:

(i). Plasma neutrino emission: Another neutrino emission mechanism, plasmon decay into a neutrino pair. This mechanism is extremely efficient at high temperatures and not too high densities in the NS crusts.

$$\gamma_{\mathrm{plasmon}} \rightarrow \nu_{\mathrm{e}} + \bar{\nu_{\mathrm{e}}}, \tag{3.2.10}$$

where γ stands for a plasmon, in the this processes, the plasmons can emit neutrinos of any favor.

(ii). Photo-neutrino emission: This process can be schematically written as

$$\gamma + \mathrm{e}^{-} \rightarrow \mathrm{e}^{-} + \nu_{\mathrm{e}} + \bar{\nu_{\mathrm{e}}}. \tag{3.2.11}$$

here γ is photon. It resembles plasmon decay but is complicated by the presence of an additional electron. The presence of an additional electron makes photo-neutrino emission more efficient than plasmon decay in a hot, low-density plasma. On the contrary, the process becomes much less efficient in a cold, high-density plasma.

(iii). Electron positron emission: This process can be written as

$$\mathrm{e}^+ + \mathrm{e}^- \rightarrow \nu_\mathrm{e} + \bar{\nu}_\mathrm{e}. \tag{3.2.12}$$

The positrons and electrons annihilate emit a pair of neutrino. This process is most efficient in the low-density and high temperature plasma, where the positron fraction is the highest. Indeed, calculations show that the process is extremely efficient in a non-degenerate plasma of temperature $\mathrm{T} \gtrsim 10^{10}$ K, which we do not study in detail. In a strongly degenerate electron plasma, the process is suppressed because of the negligibly small positron fraction.

At the very high temperatures $\mathrm{T} \gtrsim 10^9$ K found in the cores of evolved, massive stars, the dominant mode of energy loss via neutrinos is from the so-called direct URCA reactions:

$$\mathrm{n} \rightarrow \mathrm{p} + \mathrm{e}^- + \bar{\nu}_\mathrm{e},$$

and

$$\mathrm{p} \rightarrow \mathrm{n} + \mathrm{e}^+ + \nu_\mathrm{e}. \tag{3.2.13}$$

These reactions also dominate during core collapse. In both cases the nucleons in the hot interior are nondegenerate. However, when the nucleons become degenerate as in a NS that has cooled below 10^9 K, these reactions are highly suppressed. We now demonstrate this important result. Matter in the degenerate interior satisfies the

β-equilibrium condition. Beta equilibrium, in which the reaction $n \rightarrow p + e^- + \bar{\nu}_e$ is in balance with its counterpart $p + e^- \rightarrow n + \nu_e$, is set by the condition

$$\mu_n = \mu_p + \mu_e, \tag{3.2.14}$$

where μ_n, μ_p μ_e are the chemical potential of neutron, proton and electron respectively (the Fermi energy, corrected by strong interactions and very small thermal effects) of particle species i. This condition requires the fraction of protons and electrons (compared to neutrons) to be an increasing function of density [50]. Therefore neutrino production via direct URCA is possible if an exotic states are present in the core where to good approximation $[\eth(kT/\mu_n)^2]$ the chemical potentials are just the Fermi energies. Thus

$$E_F(n) = E_F(p) + E_F(e), \tag{3.2.15}$$

where $E_F(n)$, $E_F(p)$ and $E_F(e)$ are Fermi energy of neutron, proton and electron, respectively.

At the nuclear densities,

$$E_F(n) \simeq m_n c^2 + \frac{p_F^2(n)}{2m_n},$$

$$E_F(p) \simeq m_p c^2 + \frac{p_F^2(p)}{2m_p},$$

and

$$E_F(e) \simeq p_F(e)c, \tag{3.2.16}$$

here m_n, m_p, $p_F(n)$, $p_F(p)$, and $p_F(e)$ are mass of the neutron, mass of the proton, Fermi momentum of neutron, proton and electron, respectively.

Charge neutrality requires that

$$p_F(p) = p_F(e), \tag{3.2.17}$$

So Eqn. (3.2.15) reduces to

$$\frac{p_F^2(n)}{2m_n} \simeq p_F(e)c(1 + \frac{p_F(p)}{2m_p c}) - Q, \tag{3.2.18}$$

where $Q = (m_n - m_p)c^2 = 1.293$ MeV is small in comparison to the other terms in Eqn. (3.2.18). From Eqn. (3.2.18) we see that the neutron Fermi energy (minus the rest mass energy) is very nearly equal to the electron Fermi energy, i.e.,

$$E'_F(n) \equiv \frac{p_F^2(n)}{2m_n} \simeq p_F(e)c = E_F(e), \tag{3.2.19}$$

and thus

$$p_F(e) = p_F(p) \ll p_F(n), \tag{3.2.20}$$

which implies that

$$E'_F(p) \ll E'_F(n). \tag{3.2.21}$$

Let us now consider the possibility of a direct URCA reaction such as neutron decay, $n \rightarrow p + e^- + \bar{\nu_e}$ in Eqn. (3.2.13). The only neutrons capable of decaying lie within $\sim K_B T$ of the Fermi surface, with energy $E'_F(n)$. Hence, by energy conservation, the final proton and electron must also be within $\sim K_B T$ of their Fermi surfaces; the energy of escaping neutrino must also be $\sim K_B T$.

Now, according to inequality Eqn. (3.2.20), the proton and electron must have small momenta compared to the neutron. But this is impossible: the decay cannot conserve momentum if it conserves energy. In Eqns. (3.2.20) and (3.2.21), where an additional nucleon is introduced in order to guarantee momentum conservation. According to the standard cooling scenario, direct URCA process cannot occur. In order for the process to work, a bystander particle must be present to absorb momentum [51] therefore proposed that "modified" URCA reactions. Since MURCA is

less efficient than the direct URCA, the NS cooling proceeds slowly; after $\sim 10^5$ yr the photon emission becomes the dominant mechanism to lose energy.

3.3 Summery

During the neutrino cooling era, i.e., before t $\sim 10^5$ yr, the stellar cooling rate is determined by the energy loss due to neutrino emission, while during the photon cooling era, i.e. after t $\sim 10^5$ yr, it is determined by photon emission. The MURCA process dominates the blackbody emission during the neutrino emission cooling stage.

There are different neutrino emission processes. Neutrino emission is generated in numerous reactions in the interiors of NSs such as, MURCA process, and neutron-neutron and neutron-proton bremsstrahlung processes. Inside the crust, the major processes are the electron-ion neutrino bremsstrahlung process and the direct coupled electron-neutrino processes.

In the following sections we have generated the cooling rate due to these modified URCA reactions. Based on the cooling rate we have formulated the decay law and we draw a graph of ($\log$ B Vs $\log$ t).

Chapter 4

Cooling rate and magnetic field decay laws

4.1 Cooling rate

The cooling rate due to neutrino emission is normally calculated from a relation of the type.

$$\frac{\mathrm{dT}}{\mathrm{dt}} = -\frac{1}{\mathrm{q}} \int \mathrm{g}_{00}^{-1}\ \mathrm{n}\varepsilon_{\nu}\mathrm{dV_p}, \tag{4.1.1}$$

where $\mathrm{dV_p}$ is the proper volume element, q is heat capacity, g_{00} is the metric tensor, n is the baryon density and ε_{ν} is the total neutrino emissivity per baryon. If we approximate the metric tensor in Eqn. (4.1.1) to its first term as we have discussed in section (§2.2) and using Eqn. (2.2.7), hence, Eqn. (4.1.1) will reduce

$$\frac{\mathrm{dT}}{\mathrm{dt}} = \frac{1}{\mathrm{q}} \int \mathrm{n}\varepsilon_{\nu}\mathrm{dV_p}. \tag{4.1.2}$$

This integral stands for neutrino luminosity L_{ν} and the heat capacity q is given by

$$\mathrm{q} = \int \mathrm{nC}_{\nu}\mathrm{dV_p}, \tag{4.1.3}$$

here C_{ν} is the specific heat per baryon. Eqns. (4.1.1) and (4.1.2) provide the cooling law in the first 10^5 yr as [52].

The cooling equation as Shapiro and Teukolsky [47]:

$$\frac{dE}{dt} = C_\nu \frac{dT}{dt} = -(L_\nu + L_\gamma), \tag{4.1.4}$$

where E is the total thermal energy for a NS, L_ν is the total neutrino luminosity (energy transported by neutrinos per unit time) and L_γ is the total photon luminosity (energy transported by photons per unit time). In section (§3.1) we have discussed for ${L_\nu}^{\rm MURCA}$, which can be written approximately as [47]:

$${L_\nu}^{\rm (MURCA)} = 5.3 \times 10^{39}\ {\rm erg\ s^{-1}} \left(\frac{M}{M_\odot}\right) \left(\frac{\rho_{\rm nuc}}{\rho}\right)^{1/3} T_9^8. \tag{4.1.5}$$

Assuming photon emission from the surface at an effective surface temperature $T_7 = T/10^7$, we have

$$L_\gamma = 4\pi R^2 \sigma T_7^4 g_{00}^{-1}. \tag{4.1.6}$$

The total thermal energy E for a NS of mass M, density ρ and temperature T is

$$E \equiv 6 \times 10^{47}\ {\rm erg} \left(\frac{M}{M_\odot}\right) \left(\frac{\rho}{\rho_{\rm nuc}}\right)^{-2/3} T_9^2. \tag{4.1.7}$$

Inserting the above appropriate luminosities Eqns. (4.1.5) - (4.1.6) and the thermal energy Eqn. (4.1.7) in to Eqn. (4.1.4) and integrating gives the time for the star to cool from an initial interior temperature T_i to a final temperature T_f. During the neutrino cooling stage ($L_\nu \gg L_\gamma$) lasts for $t \leq 10^5$ yr; the cooling is produced by neutrino emission from the stellar interior (mainly from the core). Thus, the neutrino luminosity through in the MURCA process is calculated from

$$\frac{dE}{dt} = -L_\nu^{\rm (MURCA)}. \tag{4.1.8}$$

Substituting Eqns. (4.1.5) and (4.1.7) into Eqn. (4.1.8), we have

$$\frac{dT_9}{dt} = -\frac{1}{6}\ {\rm yr^{-1}} \left(\frac{\rho}{\rho_{\rm nuc}}\right)^{1/3} T_9^7, \tag{4.1.9}$$

where t, in this case, is in years and it will be the case for the rest of the material in the manuscript. Also in Eqn. (4.1.9), $T_9 = T/10^9$, $\rho \sim 10^{14}$ gm cm^{-3} is the average density, $\rho_{nuc} = 2.8 \times 10^{14}$ g cm^{-3} is the standard nuclear matter density.

From the above Eqn. (4.1.9) we can relate temperature T and time t as follows :

$$t - t_o = \left(\frac{\rho}{\rho_{nuc}}\right)^{-1/3} \left[\frac{1}{T_9^6(f)} - \frac{1}{T_9^6(i)}\right] \text{ yr.} \tag{4.1.10}$$

Therefore using the cooling Eqn. (4.1.9) we obtain

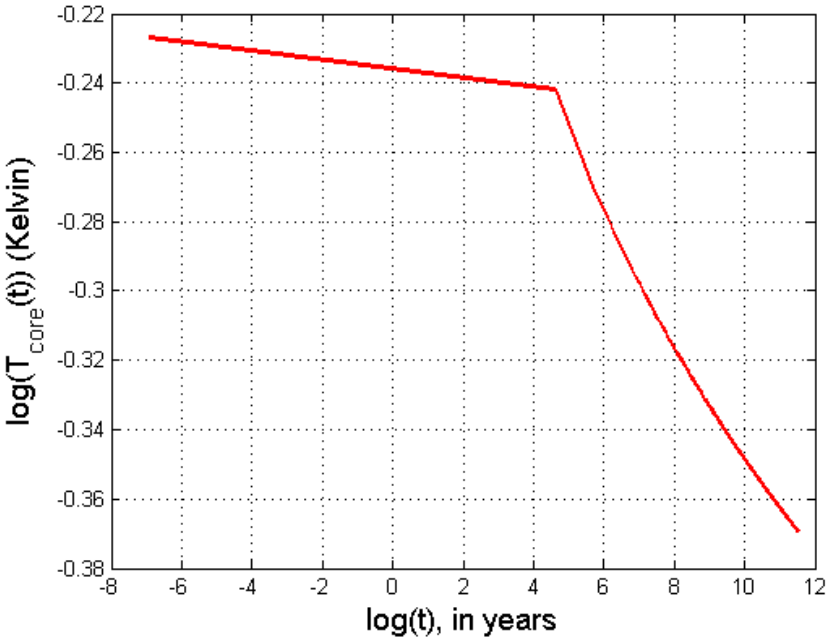

Figure 4.1: The core temperature T_{core} vs. age t relations for neutrino cooling era and photon cooling era

$$T_9 = \left[\text{yr}^{-1}\left(\frac{\rho}{\rho_{nuc}}\right)^{1/3} t + 1\right]^{-1/6}. \tag{4.1.11}$$

In Fig (4.1), the vertical line represents the core temperatures, T_{core}(in K) and the horizontal line represents time, t (in years) are shown as in logarithmic scales for the

NS cooling. The solid curve represents the cooling curve. Before the age t $\sim 10^5$ yr, the neutrino emission process dominates the photon emission process ($L_\nu \gg L_\gamma$), i.e., the star cools through neutrinos escaping from the interior (the neutrino cooling era). While after t $\sim 10^5$ yr, the photon emission process dominates the neutrino emission process ($L_\nu \ll L_\gamma$), i.e., the star cools through photons escaping from the surface (the photon cooling era).

4.2 The magnetic field decay laws

According to our new model for pulsars clearly shows that NS surface magnetic fields are spinning separated charges Q, spin frequency Ω and temperature T dependent [1].

$$B \propto \frac{Q(T)\Omega}{R\ c}. \tag{4.2.1}$$

Using Gauss's law we can calculate (-/+) charge

$$\oint \vec{E} \cdot d\vec{a} = \frac{Q}{\epsilon_o}, \tag{4.2.2}$$

here $\epsilon_o = 8.85 \times 10^{-12} \frac{C^2}{N\ m^2}$.

The magnitude of $\vec{E}$ is constant over the Gaussian surface, so it comes outside of the integral

$$\int_S \mid E \mid da = \mid E \mid \int_S da = \mid E \mid 4\pi r^2. \tag{4.2.3}$$

Thus

$$\frac{Q}{\epsilon_o} = 4\pi r^2 \mid E(r) \mid . \tag{4.2.4}$$

Substituting the electric field for spinning separated charges we have calculated in Eqn. (2.2.16) in to Eqn. (4.2.4), we obtain

$$Q = 4\pi\epsilon_o r^2 \frac{1}{\rho_{nuc}} \left(\frac{M_p^*}{M_e^*}\right)^2 \frac{K_B T_9}{\mid e \mid} \frac{\partial\rho(r)}{\partial r}, \tag{4.2.5}$$

where ρ(r) is given by [53]

$$\rho(\mathrm{r}) = \frac{3}{56\pi \mathrm{G\ r}^2}, \tag{4.2.6}$$

where G is universal gravitational constant.

$$\mathrm{Q} = -\frac{3}{7}\left(\frac{\epsilon_\mathrm{o}}{\mathrm{r\ G}\rho_\mathrm{nuc}}\right)\left(\frac{\mathrm{M_p^*}}{\mathrm{M_e^*}}\right)^2 \frac{\mathrm{K_B T_9}}{\mid \mathrm{e} \mid}. \tag{4.2.7}$$

Now we consider the dipolar magnetic field as Kebede [1].

$$\mathrm{B} = \frac{-2}{3}\frac{\mathrm{Q(T)}}{\mathrm{R}}\frac{\Omega}{\mathrm{c}}. \tag{4.2.8}$$

By substituting Eqn. (4.2.7) in to Eqn. (4.2.8) we get

$$B = \frac{2}{7}\left(\frac{\epsilon_\mathrm{o}}{\mathrm{G}\rho_\mathrm{nuc}}\right)\left(\frac{\mathrm{M_p^*}}{\mathrm{M_e^*}}\right)^2 \frac{\mathrm{K_B T_9}}{\mid \mathrm{e} \mid \mathrm{R}^2}\frac{\Omega}{\mathrm{c}}, \tag{4.2.9}$$

where r $\approx$ R.

NSs magnetic field should "decay" as a result of various cooling and braking mechanisms. NSs are known to cool as a result of neutrino and photon emission. This indicates that, there is magnetic field decay due to both, neutrino and photon emission.

Table 4.1: Field pulsars

Initial parameters	$\mathrm{B_o} = 10^{10}$ G	R = 6×10^5 cm	$\mathrm{f_o}$ = 100 Hz
Final parameters after	t $\simeq 10^9$ yr	B = 9×10^9 G	f = 90 Hz
Initial parameters	$\mathrm{B_o} = 5 \times 10^{13}$ G	R = 10^6 cm	f_o = 100 Hz
Final parameters after	t $\simeq 10^3$ yr	B = 5×10^{12} G	f = 10 Hz
	after t $\simeq 10^7$ yr	B = 5×10^{11} G	f = 1 Hz

However, there is magnetic field decay as a result of dipole magnetic radiation and quadrapole magnetic radiation. From the table (4.1), we can show that, the contributions from such braking sources as dipole magnetic radiation and the gravitational to

magnetic "decay" particularly in older pulsars (MSPs) are small as compared to that from neutrino and photon emissions and therefore are not included in our treatment. This leads to a pulsar field decay law due to magnetic braking alone results are listed in table 4.1 for those pulsars commonly referred to as field pulsars.

Our work mainly concentrates on magnetic field "decay" resulting from neutrino emission cooling sources. The standard calculations indicate that neutrino emission is the dominant cooling mechanism for up to 10^5 yr [22, 45, 52]. According to these calculations, the initial internal temperature of $T \geq 10^{11}$ K will eventually cool down to $T \sim 10^9$ K in a matter of eight hours (or 10^{-3} yr) due to intense neutrino cooling processes [47]. At this temperature the system is not only degenerate, but also cool enough to form a crystallized solid crust. So for the sake of being consistent with the original model by [3]. We have preferred to consider 10^9 K as the initial temperature for all our calculations. The magnetic field decay rate beyond this particular point in time can be estimated from the relation (ignoring the contribution from braking/spinup processes which under normal conditions are expected to be minimal). The decay rate is given by

$$\left(\frac{dB}{dt}\right)_\Omega = \left(\frac{\partial B}{\partial T_9}\right)_\Omega \times \left(\frac{dT_9}{dt}\right), \tag{4.2.10}$$

where $\frac{dT_9}{dt}$ is to be determined from the standard cooling calculations in Eqn. (4.1.9) and B is to be determined from Eqn. (4.2.9), substituting these equation, in to Eqn. (4.2.10) we get

$$\left(\frac{dB}{dt}\right)_\Omega = \frac{2}{7}\frac{\epsilon_o}{G\rho_{nuc}}\left(\frac{M_p^*}{M_e^*}\right)^2 \frac{K_B}{\mid e \mid R^2}\frac{\Omega}{c}\frac{dT_9}{dt}, \tag{4.2.11}$$

this implies that

$$\left(\frac{dB}{dt}\right)_\Omega = B_o\frac{dT_9}{dt}, \tag{4.2.12}$$

where $\mathrm{B_o} = \frac{2}{7}\frac{\epsilon_\mathrm{o}}{\mathrm{G}\rho_\mathrm{nuc}}\left(\frac{\mathrm{M_p^*}}{\mathrm{M_e^*}}\right)^2 \frac{\mathrm{K_B}}{|\mathrm{e}|\mathrm{R}^2}\frac{\Omega}{\mathrm{c}}$. Thus, integrating Eqn. (4.2.12) both sides using the appropriate terms we obtain

$$\mathrm{B} - \mathrm{B}_o = \mathrm{B_o}(\mathrm{T_9} - \mathrm{T_9(i)}), \tag{4.2.13}$$

so that

$$\mathrm{B} = \mathrm{B_o}\mathrm{T_9}, \tag{4.2.14}$$

By substituting Eqn. (4.1.11) in to Eqn. (4.2.14) according to the model adopted in this work cooling law leads to a magnetic decay law which for 10^{-3} yr $\leq$ t $\leq 10^5$ yr may be given by:

$$\mathrm{B(t)} = \mathrm{B_o}\left[1 + \mathrm{yr}^{-1}\left(\frac{\rho}{\rho_\mathrm{nuc}}\right)^{1/3}\mathrm{t}\right]^{-1/6}, \tag{4.2.15}$$

where

$$\mathrm{B_o} = \mathrm{B(t = 0\ yr)}. \tag{4.2.16}$$

The value of $\mathrm{B_o}$ could be $\geq 10^{14}$ G (depending on the initial magnitude of the separated charge, or on the initial internal temperature, or equivalently on the actual NS's mass).

The above decay law in Eqn. (4.2.15) is applicable to young NSs and from this law one can easily verify that surface magnetic fields of young pulsars will most probably be in the range of a few times 10^{12} G (Fig. 4.2). It is to be noted that the observed surface magnetic fields of active young pulsars, such as, the Crab, Vela, Geminga, PSR B1951+32, PSR B1509 - 58, PSR B1055 - 52 and PSR B1706 - 44 pulsars are within $\sim (2 - 6) \times 10^{12}$ G .

As already indicated earlier, the decay law given in eqn. (4.2.15) is associated with the first (neutrino) branch of a typical neutron star cooling curve. However, when the internal temperature falls below 10^8 K in a time window of $\sim 10^5$ yrs, photon

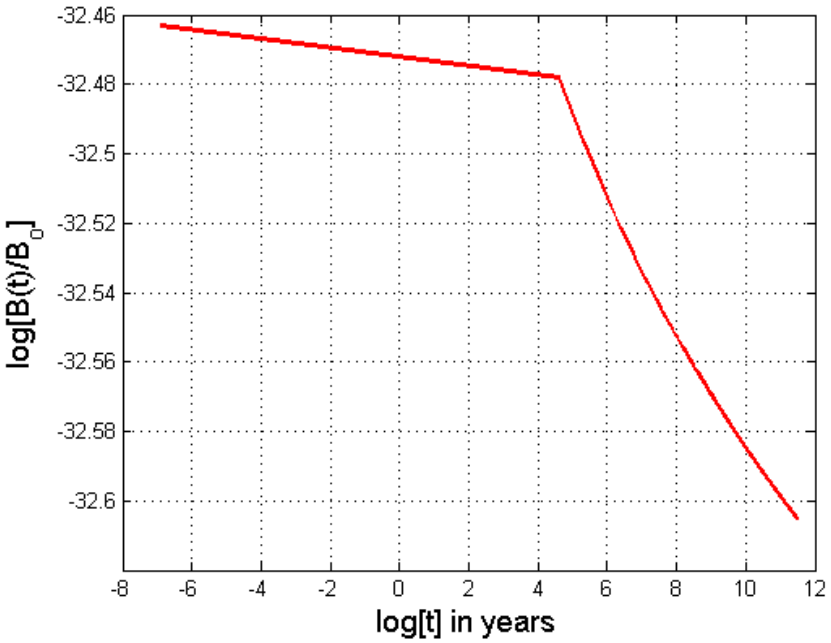

Figure 4.2: Young pulsars magnetic field decay curves due to neutrino and photon emissions

emission becomes the dominant cooling mechanism [22], for the rest of the neutron star's life [54]. This branch of the cooling curve has a slope much steeper than that of the neutrino emission branch [22].

Chapter 5

Results and discussions

Suppose t $\gg$ 1, we can relate temperature T and time t based on Eqn. (4.1.10). This implies that,

$$T_9 \propto t^{-1/6}. \tag{5.0.1}$$

According to our new model for pulsars clearly shows that NS surface magnetic field B is linearly dependent on spin frequency Ω and separated charge Q. Since this separated charge Q is also linearly dependent in the internal temperature T. Thus, based on this situation and using Eqn. (4.2.15) the surface dipolar magnetic field B and time t can be related as

$$B \propto t^{-1/6}. \tag{5.0.2}$$

The seven Gama-ray pulsars have measured values of periods P, period derivatives $\dot{P}$, spin-down luminosity $\dot{E}$, characteristics age τ_c, braking index n, magnetic field strength B. These derived parameters have obtained from different authors are shown in table (5.1). As we have shown that in Figs. (5.1), (5.2) and (5.3) the magnetic fields of the seven Gama-ray pulsars are expected to decay as a result of cooling of the NS interior. These shows that magnetic decay laws are formulated corresponding to each of the neutrino and photon branches of a standard NS cooling curve. These

Table 5.1: Magnetic field, braking index and other data of known Gamma-ray pulsars.

Name PSR	Period P(s)	$\dot{P}(10^{-13}$ s $s^{-1})$	n	$B_o(10^{13}$ G)	τ_c(kyr)	$\dot{E}$(erg s^{-1})
Crab pulsar [4]	0.033	4.23	2.52	0.76	1.3	4.5×10^{38}
Vela pulsar [30]	0.089	1.25	1.4	0.68	11	7.0×10^{36}
Geminga [55]	0.237	4.79	2.125	0.16	340	3.3×10^{34}
B1951+32 [56]	0.039	40.2	2.91	0.82	110	3.7×10^{36}
B1509-58 [31]	0.150	15.4	2.83	3.1	1.5	1.8×10^{37}
B1055-52 [55]	0.197	71.0	2.65	9.7	530	3.0×10^{34}
B1706-44 [57]	0.102			0.31	17	3.4×10^{36}

magnetic field decay are strongly linked to the long term ($\sim 10^{12}$ yr) cooling of the NS core due to neutrino and photon emissions. In the early stages of NS's life ($\sim 10^5$ yr) magnetic field decay as a result neutrino emission is dominant [22, 58, 59]. Different authors have from their simulation studies of only limited (low magnetic field pulsars) have concluded that for up to 10^8 yr pulsar fields will not decay [6]. But our work will show that the high magnetic field pulsars indeed decay during this window of time (see, Figs. (4.2), (5.1) and (5.2)).

From Fig. (5.3) we have sampled the objects in three groups according to their measured magnetic field: high field NSs with $B_o \geq 10^{14}$ G, intermediate field NSs with 10^{13} G $< B_o < 10^{14}$ G and low field NSs for which $B_o < 10^{13}$ G. We found that this three samples could be explained qualitatively by cooling curves in three different regimes: high, intermediate and low magnetized NSs, in all cases their magnetic field decrease with time. These pulsars have measured values of periods, period derivatives, spin-down luminosity, characteristics age, braking index, magnetic field strength. The derived parameters of this analysis are shown in table (5.1).

The decay law given in Eqn. (4.2.15) is already indicated to provide results which are in excellent agreement with observations. This has paramount importance in determining the nature of the time evolution of pulsar's magnetic fields across all

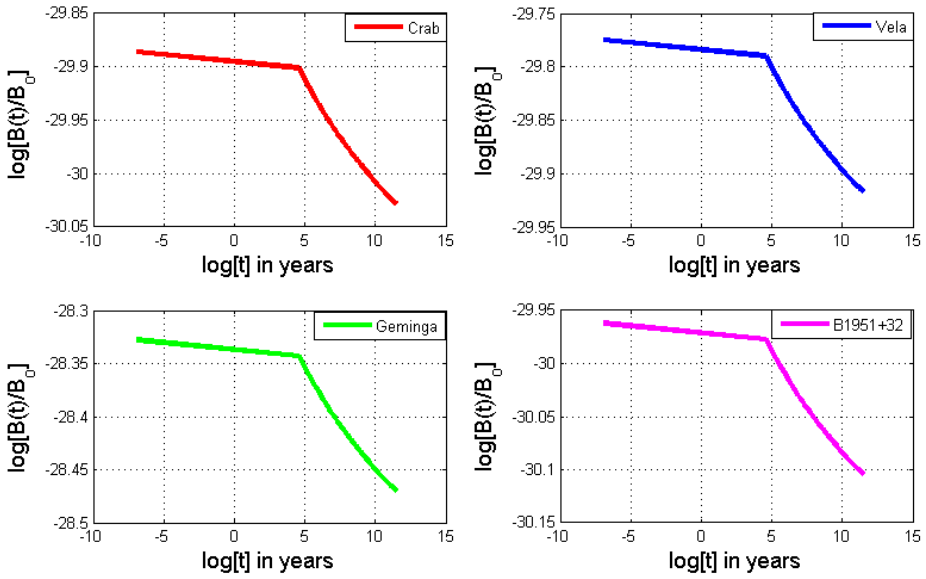

Figure 5.1: The Crab, Vela, Geminga and PSR B1951+32 pulsars magnetic field decay curves due to neutrino and photon emissions

age domains. Moreover, this law provides the means for the analytic solution of the pulsar spin down law, i.e.,

$$\dot{\Omega} = \Lambda(t)\Omega^{n}, \tag{5.0.3}$$

where $\Lambda(t)$ is time dependent and n is for the braking index. [32] have attempted to address the issue of pulsar braking index variations from the expected value of n = 3 (for electromagnetic braking) [60] in terms of secular increase in the magnetic moment. For example, [61] have shown that the magnetic field increases following the relation,

$$B \propto t^{1/6}. \tag{5.0.4}$$

as proposed by [2] predicts a braking index for the Crab pulsar which is in good agreement with the observed value. Actually, it can be shown that for the measured

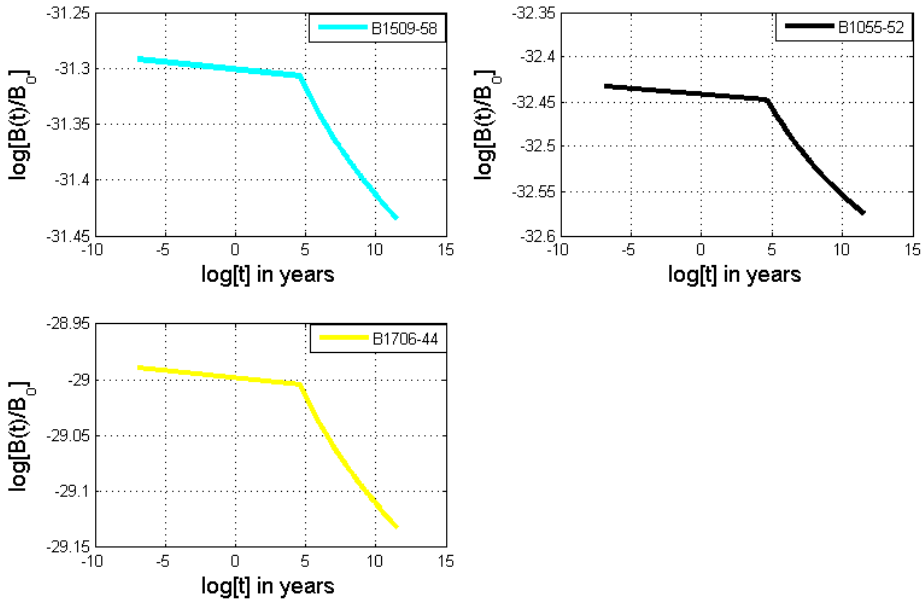

Figure 5.2: The PSR B1509-58, PSR B1055-52 and PSR B1706-44 pulsars magnetic field decay curves due to neutrino and photon emissions

values of Ω and $\dot{\Omega}$ the decay law given in Eqn. (4.2.15) also provides a braking index of 2.52 for the Crab pulsar. However, the advantage of having to work with this decay law Eqn. (4.2.15) is that using this law the time evolution of the braking index for any one given pulsar can now be roughly determined for any age of the pulsar provided the current values for Ω and $\dot{\Omega}$ are precisely known. This is something which is not possible to get from the model proposed by [2] due to the time constraint of 10^3 yrs it imposes.

Though it is not our intention to go into details, but we like to point out that the nature of the time evolution of braking indices, according the model adopted in this work is very much complicated by such mechanisms as quadrupole gravitational and magnetic dipole radiations as well either spin down or spin up the pulsar but

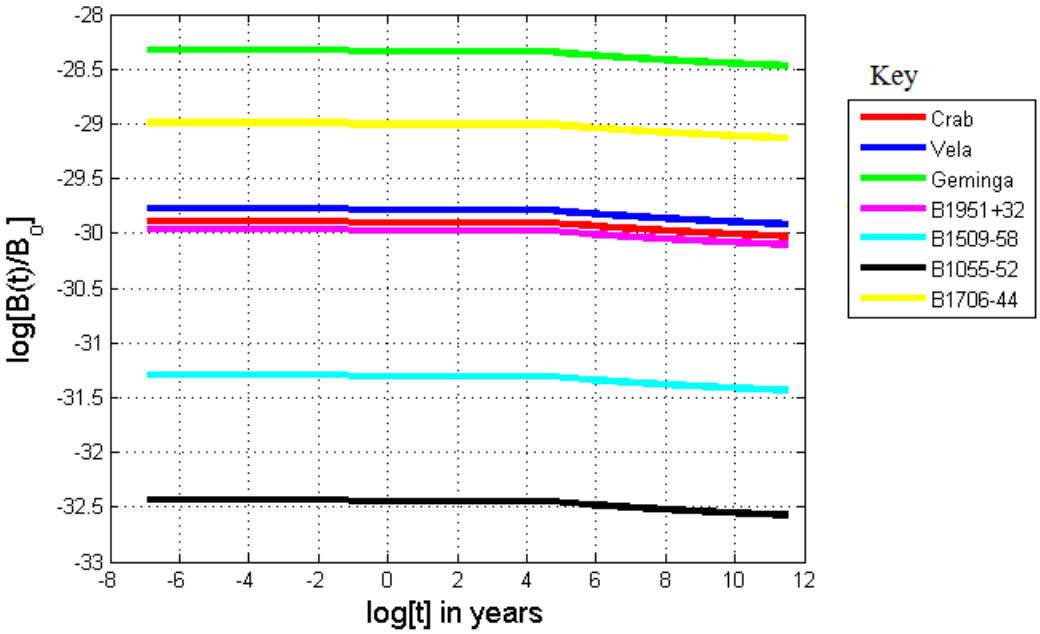

Figure 5.3: The known Gamma-ray pulsars magnetic field decay curves due to neutrino and photon emission processes.

also at the same time decrease or increase the intensity of the surface magnetic fields respectively. Even though the magnetic decay (or revival) law resulting from these are not expected to be that significant. Obviously, then the combination any number of these in various proportions along with the main magnetic decay law given in Eqn. (4.2.15) may result in randomized braking indices.

Chapter 6

Conclusions

So far there is no clear understanding of how pulsar magnetic fields decay. Investigations also indicate that no significant magnetic decay occurs in a NS's life time [5, 6]. This has raised a number of open problems on how magnetic moments for example, the so called milli-second-pulsars decay from a typical value of $\sim 10^{30}$ G cm^3 down to 10^{25-26} G cm^3 in a time window of about 10^{7-8} yr [6, 7, 8, 9].

To answer such questions we consider spinning separated charges are most likely source for NS magnetic field. In this model of the NS surface magnetic fields are not only identified as dipolar but also shown to be temperature dependent as was derived in Eqn. (4.2.5) and Eqns.(4.2.7 - 4.2.9), respectively.

The emission of neutrinos take place in the core of NSs during the predominant cooling stage immediately after its formation. Even though there are various neutrino emitting reaction, we have emphasis to the modified URCA reaction. The cooling from such a reaction is strongest during the first 10^5 yrs. We have seen that NS loses its energy and is observed to cool, as a result of neutrino emission from the core and photon emission from the surface. The most effective cooling process at t $\lesssim 10^5$ yrs will be the neutrino emission during the modified URCA reaction and the photon

emission overtakes the neutrino on the NS when t $\gtrsim 10^5$ yrs.

We have already derived the magnetic decay law for young pulsars like Crab, Vela, Geminga, PSR B1951+32, PSR B1509-58, PSR B1055-52 and PSR B1706-44 (known Gamma-ray pulsars), which are governed in Eqn. (4.2.15). Our work have been shown that pulsars magnetic field indeed decay during this window of time. As we have shown that from Figs. (4.2), (5.1), (5.2)and (5.3) the surface fields of young pulsars are also expected to decay via neutrino and photon emission mechanism, which is different among others decay processes, like Ohmic decay. However, our target in this work is magnetic field decay via neutrino emission mechanism. As such, we found the expression for time evolution of the internal temperature of NSs (temperature T versus time t), when t $\gg 1$ in Eqn. (4.1.11) to be T $\propto t^{-1/6}$. The actual decay law, in this case, can be formulated based on the fact that, for this branch, the first segment of the slope of the cooling curve in a (log T , log t) plot is $\sim -1/6$. This clearly show that, the present model for magnetic field decay is strongly linked to the long term $\sim 10^5$ yr cooling of the NS core as was shown in our derivation of the 'decay law' of Eqn. (4.2.15). Based on this situation, it is clearly indicates that, when t $\gg 1$, then B $\propto t^{-1/6}$. The second segment of the decay law, on the other hand, is expected to involve a much faster decay rate as compared to the first. This is due to the strong surface fields which naturally tend to enhance cooling by photons [22].

We suggest that further research in this direction is likely going to reveal additional properties of pulsars magnetic field decay law of NSs via photon emission and these contributes to our understanding how such magnetic field decays as a result of photon emission will be prominent for about after 10^5 yr.

Bibliography

[1] Kebede, L. W., 2002, Astrophys. and Space Sci., **282, 131**

[2] Blandford, R. D., Applegate, J. H. and Hernquist, L., 1983, MNRAS, 204, 1025

[3] Kebede, L. W., 1996, MNRAS, **282, 845**

[4] Manchester, R. N. and Taylor, J. H., 1977, Pulsars, Freeman, New York

[5] Narayan, R. and Ostriker, J. P., 1990, ApJ, **352 222**

[6] Bhattacharya, D., Wijers, R., Hartman, J. and Verbunt, F., 1992, A and A **254, 198**

[7] Bhattacharya, D., Van den Heuvel, E. P. G., 1991, Phys. Rev., **203,1**

[8] Hartman, J. W., Verbunt, F., Bhattacharya, D. and Wijers, R., 1997, A and A.

[9] Burderi, L. and D' Amico, N., 1997, ApJ, **490, 343**

[10] Verbunt, F., 1994, in AIP Conf. Proc. 308, The evolution of X-Ray

[11] Sangupta, S., 1997, ApJ, **479, L133**

[12] Shibazaki, N., Murakami, T., Shaham, J. and Nomoto, K., 1989, Nature, **342, 703**

[13] Geppert, U. and Uprin, V. A., 1994, MNRAS, **271, 490**

[14] Michael, F. C., 1991, *Theory of Neutron Star, Magnetospheres (Chicago Press)*

[15] Hewish, et., al., A., 1968, Nature 217, 709

[16] Robert, C. Duncan, May, 1998, Updated March, 2003

[17] Truemper, J., Pietsch, W., Reppin, C., et., al., 1978, ApJ, 219, L105

[18] Bisnovatyi-Kogan, G. S., Komberg B. V., 1975, Soviet Astron., 18, 217

[19] Murakami T., et., al., 1988, Nature, **335, 234**

[20] Phinney, E. S. and Kulkarni, S. R., 1994, ARA and A, **32, 591**

[21] Gunn, J. E. and Ostriker, J. P., 1970, ApJ, **160, 979.**

[22] Glen G. and Sutherland P., 1980, *On the cooling of neutron stars.* Astrophysical Journal, **239:671**

[23] Gold, T. *Rotating neutron stars as the origin of the pulsating radio sources. Nature,* **218:731, 1968**

[24] Lyne, A. G., Graham-Smith, F., 1998, *Pulsar Astronomy 2nd ed. (Cambridge: Cambridge Univ. Press)*

[25] Malov, I. F., 2004, Radiopul'sary (Radiopulsars) (Moscow: Nauka)

[26] Thompson, D. J., 2001, *In High Energy Gamma-Ray Astronomy, American Institute of Physics (AIP) Proceedings, 558, Edited by Felix A. Aharonian and Heinz J., Volk. American Institute of Physics, Melville, New York, p.***103-114**

[27] Glendenning, N. K., 2000, *Compact Stars, 2nd ed. (Springer, New York).*

[28] Jackson J. D., 1991, *Classical Electrodynamics,3d. ed (New York: Wiley)*

[29] Lyne, A. G., Pritchard, R. S. and Smith, F. G. 1993, MNRAS, **265, 1003**

[30] Lyne, A. G., Pritchard, R. S., Graham-Smith, F. and Camilo, F., 1996

[31] Kaspi, V. M., Manchester, R., Siegman, B., Johnston, S., and Lyne A. G., 1994, ApJ, **422, L83**

[32] Blandford and Romani, R. W., 1988, MNRAS, **234**, Short Communication 57p

[33] Kaspi, V. M., 2010, Publ. Nat. Ac. Science, **107, 7147**

[34] Manchester R. N., Hobbs, G. B., Teoh, A., Hobbs, M., 2005, AJ, **129, 1993**

[35] Brooker, G. A. and Skyes, J., 1968, Phys. Rev. Lett., **21, 279**

[36] Andersen, R.H. and Pethick, C.J. and Quader, K. F., 1987, Phys. Rev. B, **35, 1620**

[37] Weinberg, S., 1972, *Gravitation and Cosmology, Wiley, New York*

[38] Gunn, J. E., Ostriker, J. P., 1969, Nature, **221, 45**4

[39] Mekuanint, K., 2007, M. Ss. thesis, Addis Ababa Univ.

[40] Manchester, R. N., Durdin, J. M. and Newton, L. M., 1985, Nature, 313, 374

[41] Oliva, J. and Ashcroft, N. W., 1982, Phys. Rev. B, **25, 223**

[42] Jackson, J. D., 1975, *Classical Electrodynamics, 2nd. ed. (New York: Wiley)*

[43] Tsuruta, S., 1964, PhD. thesis, Columbia University.

[44] Reisenegger, A., 2009, **499, 557**

[45] Tsuruta, S., 1974, in IAU Symposium 53, Physics of Denser Matter

[46] Tsuruta, S., 1979, Phys. Rept., **56, 237**

[47] Shapiro, S.L. and Teukolsky, S. A., 1983, *Black Holes, White Dwarfs and Neutron Stars, (Wiley-Interscience, New York).*

[48] Pethick, C. J., 1992, *Cooling of neutron stars, Rev. Mod. Phys.* **64, 1133, 1140**

[49] Friman, B. L., and Maxwell, O. V., 1979, ApJ., **232, 541**

[50] Pethick, C. J., 1991, preprint

[51] Chiu, H. Y., and Salpeter, E. E., 1964, Phys. Rev. Letters, **12, 413C.**

[52] Bachall, J. N., and Wolf, R. A., 1965, Phys. Rev. B, **140, 1452**

[53] Meisner, C. W. and Zapolsky, H. S., 1964, Phys. Rev. Lett., **12, 635**

[54] Baym, G., and Pethick, C., 1979, Ann. Rev. astron. Astrphys., **17, 415**

[55] De Luca, A., Caraveo, P. A., Mereghetti, S., Negroni, M., and Bignami, G. F., 2005, ApJ, **623, 1051**

[56] Hartman, R. C., Bertsch D. L., Bloom S. D., Chen A. W., Deines-Jones P., et al., 1999, ApJ, **123, 79**

[57] McGowan, K. E., Zane, S., Cropper, M., Kennea, J. A., Cordova, F. A., Ho, C., Sasseen, T. and Vestrand, W. T., 2004, ApJ, **600, 343**

[58] Nomoto, K., Tsuruta S., 1981, ApJ, **250, L19**

[59] Van Riper, K. A., Lamb, D. Q., 1981, ApJ, **244, L13**

[60] Goldreich, P., Pacini,F. and Rees, M J., 1971, Astrophys. Space Sci., **3, 185**

[61] Chanmugam, G. and Sang, Y., 1989, MNRAS, **241, 295**

Declaration

This thesis is my original work, has not been presented for a degree in any other University and that all the sources of material used for the thesis have been duly acknowledged.

Name: Tsegay Bezabh Buru

Signature:

Place and time of submission: Addis Ababa University, October, 2017.

This thesis has been submitted for examination with my approval as University advisor.

Name: Dr. Remudin Reshid

Signature: